Unimer Exchange Is not Necessary for Morphological Transitions in Polymerization-Induced Self-Assembly

Clément Debrie, Noémie Coudert, Jean-michel Guigner, Taco Nicolai, François Stoffelbach, Olivier Colombani, Jutta Rieger

COMMUNICATION

Unimer Exchange is not Necessary for Morphological Transitions in Polymerization Induced Self-Assembly

Clément Debrie,[a] Noémie Coudert,[b] Jean-Michel Guigner,[c] Taco Nicolai,[b] François Stoffelbach,[a] Olivier Colombani*[b] and Jutta Rieger*[a]

[a] C. Debrie, Dr. F. Stoffelbach, Dr. J. Rieger
Sorbonne Université & CNRS (UMR 8232)
Institut Parisien de Chimie Moléculaire (IPCM), Polymer Chemistry Team
4 Place Jussieu, 75252 Paris Cedex 05, France
E-mail: jutta.rieger@sorbonne-universite.fr

[b] N. Coudert, Dr. T. Nicolai, Dr. O. Colombani
Le Mans Université & CNRS (UMR 6283)
Institut des Molécules et Matériaux du Mans (IMMM)
Avenue Olivier Messiaen, 72085 Le Mans Cedex 9, France

[c] Dr. J.-M. Guigner
Sorbonne Université, MNHN, CNRS UMR 7590
Institut de Minéralogie, de Physique des Matériaux et de Cosmochimie (IMPMC)
IRD, 75252 Paris Cedex 05, France

Supporting information for this article is given via a link at the end of the document.

Abstract: Polymerization-Induced Self-Assembly (PISA) has established itself as a powerful and straightforward method to produce polymeric nano-objects of various morphologies in (aqueous) solution. Generally, spheres are formed in the early stages of polymerization that may evolve to higher order morphologies (worms or vesicles), as the solvophobic block grows during polymerization. Hitherto, the mechanisms involved in these morphological transitions during PISA are still not well understood. Combining a systematic study of a representative PISA system with rheological measurements, we demonstrate that - unexpectedly - unimer exchange is not necessary to form higher order morphologies during radical RAFT-mediated PISA. Instead, in the investigated aqueous PISA, the monomer present in the polymerization medium is responsible for the morphological transitions, even though it slows down unimer exchange.

Polymerization-Induced Self-Assembly (PISA) has been widely studied during the last 15 years[1,2]. It consists in simultaneously synthesizing and self-assembling amphiphilic block copolymers (ABC) in a selective solvent of one of the blocks, typically water, to prepare nano-assemblies at high solids contents through a straightforward and green process. Not only spheres can be prepared, but also higher order morphologies (such as worms or vesicles). The latter are of particular interest because they find use in many applications, for instance as viscosity modifiers or soft hydrogels (worms)[3], as nanoreactors[4] and as drug delivery systems (vesicles)[5,6]. For diblock copolymers, the morphology is thermodynamically dictated by the packing parameter[7] which is defined as $p = V/(a \cdot l)$ where V is the volume occupied by the solvophobic B block, l its length and a the contact surface between the two blocks. As the size of the B block increases during polymerization, so does p. Therefore, higher order morphologies should eventually always be obtained in PISA from a thermodynamic point of view, at least for short and uncharged solvophilic blocks[8,9].

However, in the literature there are many examples where only spherical nano-objects have been obtained despite a favorable block length ratio, which suggests kinetic hurdles preventing reorganization to higher order morphologies[10–14]. The fact that most nano-objects at the end of PISA are out-of-equilibrium (= frozen) due to kinetic constraints is confirmed by the role of the preparation route on the obtained morphologies. For instance, Ferji *et al.* demonstrated that glycopolymer self-assemblies exhibited different morphologies when prepared via PISA or via nanoprecipitation.[15] It was also reported that the initiation system used in PISA[16,17], which affects the end-group fidelity and kinetics of polymerization, can impact the particle morphology even though it should not have any influence on the thermodynamics of self-assembly.

Higher order morphologies (worms, vesicles) have been produced with various polymers. Kinetic monitoring of the PISA process in these cases revealed that spheres are formed at the early stages of the polymerization and then transform into other morphologies[18,19]. This implies that reorganization of the AB diblock copolymers occurs at some point. A key question remains however unanswered: What are the processes involved in PISA that promote the reorganization of nano-assemblies into higher order morphologies?

Generally, two main processes take place during self-assembly of ABC[20–22]: unimer exchange[23,24] and fusion/fission[25–27]. The former involves the displacement through the aqueous medium of a single polymer chain (unimer) from one solvophobic core to another. The energy barrier for such exchange depends on the mobility, hydrophobic character and length of the B block. Fission or fusion of self-assemblies is usually considered unlikely for ABC, at least at low concentration, because of the steric hindrance caused by the corona[28,29]. The fact that the morphologies depend on the preparation pathway for the same final conditions implies that unimer exchange is generally inhibited at the end of PISA. Otherwise, the same thermodynamic equilibrium would be reached no matter the pathway. However, since the B block grows during the polymerization and monomer is present during PISA, it is possible that unimer exchange occurs up to some point during the process, allowing morphological transitions, but eventually becomes too slow.

In this communication, we study a typical Reversible Addition-Fragmentation Chain-Transfer Polymerization (RAFT)-PISA system in water, and investigate for the first time the role of unimer exchange in morphological transitions during PISA. Our strategy is to monitor the morphological transitions during PISA and to correlate this to the rate of unimer exchange. 2-Methoxyethylacrylate (MEA) was chosen as a model monomer to build the hydrophobic block while possessing a good water solubility. MEA has already been studied as a core-forming monomer in PISA[8,30–32], but the variability of the obtained self-assemblies makes a study of its re-organizations and dynamics even more interesting and valuable. PMEA has a low glass transition (T_g(PMEA) ≈ - 50 °C)[33] and its rate of unimer exchange has recently been shown to strongly depend on its molar mass[34], making this polymer a good candidate for our study.

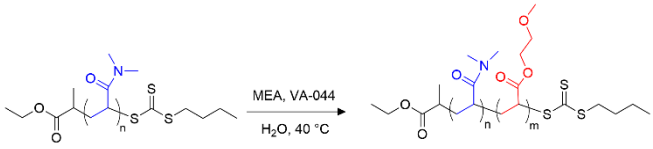

Scheme 1. Chain extension of the PDMAc macroCTA to form PDMAc-*b*-PMEA diblock copolymers by aqueous PISA.

In order to produce PDMAc-*b*-PMEA amphiphilic diblock copolymer assemblies by RAFT-mediated PISA in water, water-soluble PDMAc macromolecular RAFT agent (macroCTA) (with DP_n = 24, see SI section 3.a) was chain extended in aqueous PISA with MEA (see ***Scheme 1*** *and Scheme S1*). The reaction was conducted at 40 °C using VA-044 ($t_{1/2}$ (40 °C) ~ 16.5 h)[35] as a radical initiator, because preliminary tests showed that a better control was achieved at moderate temperature[30] where transfer and recombination reactions are disfavoured. The initial monomer concentration was set to 1.5 M (final solids contents ~ 20 wt%). In these conditions, the initial reaction medium was biphasic because the solubility of MEA in water at 40°C is equal to 11 wt%. As reported in *Table S2*, the samples are named P*R*, where *R* corresponds to the targeted number-average degree of polymerization, DP_n, of the hydrophobic PMEA block at 100% conversion. *R* was systematically increased by varying the initial monomer to macroCTA molar ratio, $[MEA]_0/[CTA]_0$ (= *R*), from 150 to 400 in order to study its impact on the obtained morphologies. All polymerizations reached high monomer conversion (> 92%) and were well-controlled: size exclusion chromatography (SEC) revealed low dispersities (*Đ* < 1.2) and quantitative chain extension of the macroRAFT agent (*Figure S2*).

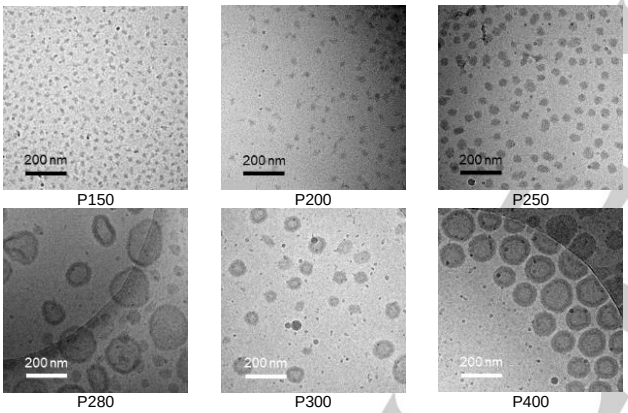

Figure 1. Representative cryo-TEM pictures of the final diblock copolymer dispersions diluted to 3 wt% synthesized at various $[MEA]_0/[CTA]_0$ = R (*Table S2*). The dark spots are surface contaminations stemming from water crystals.

As observed by cryo-TEM (***Figure 1***), the minimum *R* necessary to obtain higher order morphologies close to full conversion is situated between 250 and 280. Indeed, the final morphologies were spheres for *R* ≤ 250, a mixture of vesicles and smaller objects for *R* = 280, and vesicles were formed for *R* = 300 and 400. The cryo-TEM pictures are consistent with the visual aspect of the polymer dispersions: P150 is a translucent yellowish liquid; the dispersions become more and more turbid with increasing *R*, whereas all vesicle dispersions (P300 and P400) are milky and liquid. No worms were observed in the studied experimental conditions. This might be explained by the fact that the compositional window where worms can be found is generally very narrow[8,36–38] and was apparently not covered in this set of experiments. Worms were actually observed in other conditions (see below, Mz series).

We showed that vesicles were obtained for *R* ≥ 280. In order to determine whether the formation of higher order morphologies was only controlled by the final DP_n of the B block or by additional parameters, we monitored the morphologies as a function of conversion. *R* = 400 (see *Table S3*) was chosen, as it should allow us to determine the morphologies over a large range of DP_n. Kinetic monitoring of typical PISA formulations, in particular by *in situ* SAXS analyses[18,19], has already been described for other copolymers, but the driving force for the observed morphological transitions has not been identified yet. The samples taken from the reaction medium during polymerization were named M*z-conv.*, where *z* indicates the reached DP_n at the given monomer conversion in %. The polymerizations were well controlled as shown by the progressive shift of the SEC signals towards higher molar masses and the disappearance of the macroCTA (*Figure S4*).

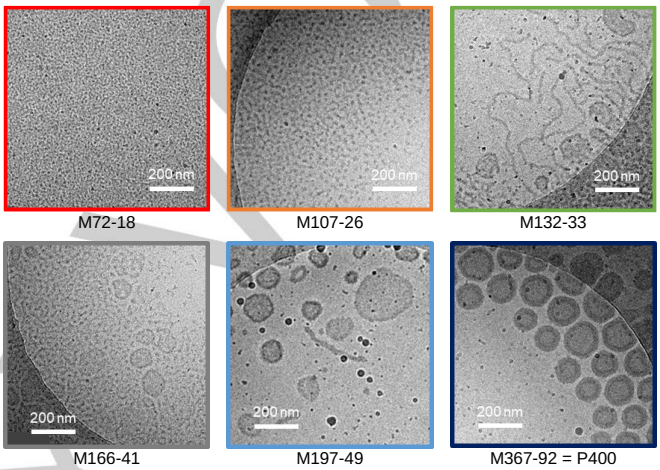

Figure 2. Representative cryo-TEM pictures of samples M*z-conv.*, see *Table S3*.

A preliminary investigation of the evolution of the morphologies during PISA was first conducted by dynamic light scattering (DLS, see SI, section 4.b), before imaging the most relevant kinetic samples by cryo-TEM (***Figure 2***). Spheres were obtained at least up to $DP_{n,B}$ = 72 (sample M72-18). During the polymerization, the spheres then quite quickly evolved and led to a mixture of morphologies. In M107-26, a majority of spheres and short worms (L < 100 nm) were observed. This confirmed that a transition from spheres to cylinders occurred before further evolution towards vesicles, as expected[7]. In sample M132-33, spheres, vesicles and long fibers (several hundreds of nm long) were obtained. The morphological transitions continued, passing through a mixture of spheres, short worms and vesicles in quasi identical proportions (M166-42), a mixture of mainly vesicles with a few worms (M197-49) and finally only vesicles (M367-92).

Strikingly, for comparable $DP_{n,B}$, *i.e.* PMEA block length reached, there is a strong difference in morphology between the self-assemblies obtained at quasi full monomer conversion (series P*R*) and at intermediate conversion (series M*z-conv.*), see *Figure S5.* For example, M132-33, M166-41 and P150, at 33%, 41% and 95% conversion respectively, have comparable $DP_{n,B}$ but P150 consisted only of small spheres, whereas the two others contained a mixture of spheres, worms and vesicles. Similarly, P200 (at 95% conversion) contained only spheres, whereas vesicles and a few long worms were observed in M197-49. Thus, it seems that a smaller hydrophobic block is required to trigger morphological evolutions during PISA than at full conversion. Such discrepancy was already observed by Sumerlin *et al.*[19] using diacetone acrylamide as a hydrophobic monomer, but the origin of the difference between full conversion morphologies and their appearance during PISA was not discussed. Two major differences exist between series P*R* and M*z-conv.*: because of the incomplete monomer conversion in the latter series, the total polymer solids content is lower and a large amount of residual monomer is still present.

It is now clear that PDMAc-*b*-PMEA copolymers with $DP_{n,B} \geq 100$ can form higher order morphologies and that the morphological transitions are not only influenced by the actual $DP_{n,B}$, but also by the conversion at which it is reached. This implies that the concentration of free monomer, of polymer or both may be a key parameter that favors morphological transitions. In order to rationalize these results, the kinetics of unimer exchange were determined in the absence or presence of MEA monomer.

Different strategies exist to estimate the rate of unimer exchange for self-assembled amphiphilic block copolymers in solution.[20] One reliable strategy consists in the synthesis of BAB triblock copolymers possessing a central hydrophilic A block and two lateral hydrophobic B blocks. At sufficiently high concentration (percolation concentration, C_p), the polymers self-assemble into a transient network consisting of hydrophobic cores containing the B blocks, surrounded by bridges of A blocks. This physically cross-linked network is able to relax provided that the B blocks exchange between different cores. The rheological response of the network therefore gives a quantitative estimation of the exchange rate of the B blocks[39–41]. In order to estimate the exchange rate of the B blocks, we therefore studied $PMEA_x$-*b*-$PDMAc_{400}$-*b*-$PMEA_x$ BAB triblock copolymers by oscillatory linear rheology[42,43] in aqueous medium[34].

It should be noted that at concentrations slightly above C_p super-bridges (defects in the network) may cause the measured rheological relaxation time to be much lower than the actual exchange time of the B blocks.[39] On the contrary, Zinn *et al.* showed that at concentrations sufficiently above C_p, the terminal relaxation time measured by rheology for transient networks formed by BAB triblocks is quantitatively identical to the exchange time (τ_R) of B blocks measured for AB diblock copolymers assemblies in dilute solution.[41] Rheology experiments were therefore conducted above 70 g/L to give a more realistic estimation of the exchange time of the B blocks in the PISA conditions. Additionally, we stress that we chose a long PDMAc block ($DP_{n,A} \approx 400$) on purpose for the BAB triblocks to reduce C_p and favor the formation of spherical assemblies, which facilitates the quantification of the exchange dynamics by rheology. The exchange rate of B blocks is actually mainly controlled by the length and composition of these blocks with little influence of the length of the hydrophilic A block[42,43]. Therefore, the exchange times measured by rheology on $PMEA_x$-*b*-$PDMAc_{400}$-*b*-$PMEA_x$ trustworthily inform on the exchange time of diblock copolymers consisting of B blocks with the same DP_n but shorter A blocks in the conditions of the PISA polymerizations.

We have recently measured the exchange time of PMEA blocks as a function of T and $DP_{n,B}$ = x = 50, 100, 200) for $PMEA_x$-*b*-$PDMAc_{400}$-*b*-$PMEA_x$ triblock copolymers in aqueous solution (without additional MEA monomer) (***Figure 3a***).[34]

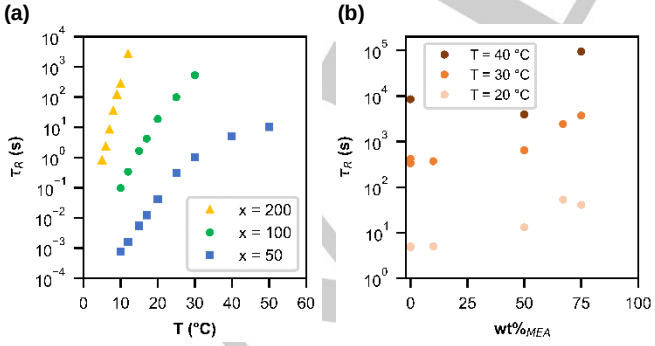

Figure 3. (a) Relaxation time as a function of temperature for triblock copolymers $PMEA_x$-*b*-$PDMAc_{400}$-*b*-$PMEA_x$, where x = 50, 100 and 200 (C = 100 g/L). (b) Relaxation time as a function of MEA weight fraction ($wt\%_{MEA} = m_{free\ MEA}/(m_{free\ MEA} + m_{B\ block})$) for x = 100 (C = 70 g/L) at different temperatures.

Briefly, it was observed that the exchange time increases with x, which can be explained by a decrease in mobility and an increase of the surface area of contact with water as the B block becomes longer[20,42]. Moreover, the exchange time progressively increases with temperature no matter x, which is opposite to a classical Arrhenian behavior and was attributed to the fact that the PMEA blocks dehydrate with increasing temperature. ***Figure 3a*** summarizes the evolution of the exchange time as a function of T for the different x.[†]

In PISA, free monomer, swelling the hydrophobic cores, was suggested to have a plasticizing role, promoting morphological transitions[44] through enhanced chain mobility and, as a consequence, an increased unimer exchange rate. To check this hypothesis, the rheological properties of $PMEA_{100}$-*b*-$PDMAc_{400}$-*b*-$PMEA_{100}$ were investigated at C = 70 g/L between 20 and 40 °C in the presence of increasing amount of MEA, mimicking various monomer conversions during PISA ($wt\%_{MEA} = m_{free\ MEA}/(m_{free\ MEA} + m_{PMEA}) = m_{free\ MEA}/m_{total\ MEA}$ varying between 0 and 75 $wt\%_{MEA}$). Very surprisingly, the exchange dynamics was slowed down in the presence of monomer. Indeed, τ_R increased with the monomer content up to one order of magnitude (see ***Figure 3b***). This behavior might be explained by the fact that MEA swells the hydrophobic core, replacing partially the water hydrating the PMEA blocks, making them even more hydrophobic.

In the PISA experiment with R = 400, morphological transitions were first observed for M107-26, that is for $x \approx 100$, *i.e.* in the presence of approximately 75 $wt\%_{MEA}$. At 30 °C and with such a high MEA content, τ_R is already close to an hour (see ***Figure 3b***). The polymerizations were actually conducted at 40 °C, where τ_R is even higher[†] (see ***Figure 3***). In view of the polymerization kinetics (*Figure S3*), which are rapid compared to those exchange rates, it is clear that any morphological transitions occurring during PISA for monomer conversions higher than 25% cannot result from unimer exchanges.[‡] We therefore demonstrated that the exchange of unimers is not responsible for morphological transitions and that the free monomer is actually not accelerating the dynamics of unimer exchange. This leads us to conclude that fusions of primary aggregates are necessarily involved in the morphological transitions. However, the role of the monomer in the formation of worms/vesicles is still unclear.

Interestingly, it has been proposed in the literature that the presence of solvent, monomer or molecules with similar chemical structure may help morphological transitions[44–50]. On the one hand, we have demonstrated that the presence of toluene in a typical emulsion polymerization of styrene via PISA has a great impact on the morphologies formed;[50] on the other hand, the addition of plasticizing solvents post-polymerization (to particles obtained by PISA or mini- or nanoemulsion) was extensively explored by the groups of Davis[44] and Anastasaki[45]. For instance, the latter showed that the addition of toluene in an aqueous dispersion of nano-objects comprising a polystyrene solvophobic block can trigger quick transitions toward higher order morphologies.

In order to assess the role of MEA on the morphological transitions observed during PISA, we added varying quantities of MEA, post-polymerization, to sample P200 that was diluted to 5 wt%. As a reminder, this sample contained only spherical particles. Visually, an increase in turbidity was instantaneously observed upon the addition of 50 to 70 $wt\%_{MEA}$ (leading to a solvent composition of around 5-11 $vol\%_{MEA} = V_{free\ MEA} / (V_{free\ MEA} + V_{water})$). Cryo-TEM was used to detect any morphological changes (***Figure 4***). Unlike the pristine sample containing 4 $wt\%_{MEA}$, the samples obtained upon addition of 22 $wt\%_{MEA}$ already contained some short worms (see ***Figure 4***). The objects further evolved into a mixture of vesicles, worms and spheres (with similar sizes around 100 nm) at 32 $wt\%_{MEA}$ and to only vesicles at 72 $wt\%_{MEA}$ (accounting for the visually observed increase in turbidity). We suppose that the formation of worms and/or vesicles happens quasi-instantaneously: the increase of turbidity was immediately detected after the addition of MEA to reach ~ 50 $wt\%_{MEA}$.

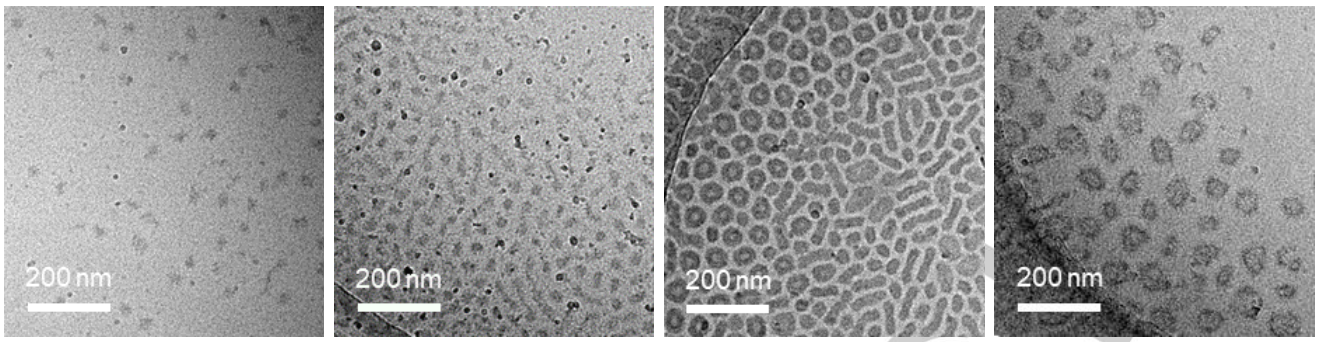

(a) 4 wt%*$_{MEA}$ (b) 22 wt%$_{MEA}$ (c) 32 wt%$_{MEA}$ (d) 72 wt%$_{MEA}$

Figure 4. Representative cryo-TEM pictures of P200 dispersions recorded at 3 wt% to which increasing amounts of MEA were added (see *Table S4*). *residual MEA after PISA.

Considering that the unimer exchange is extremely slow in these conditions ($\tau_R > 10^4$ s at 20 °C even without monomer, see ***Figure 3b***), we can conclude that these morphological transitions originate from the fusion of the spherical particles triggered by the sole addition of monomer.

We hypothesize that the addition of monomer increases the volume of the hydrophobic cores by swelling them and therefore favors higher order morphologies (increase in packing parameter). It is quite unlikely that the free MEA plays a crucial plasticizing role on the PMEA cores (which would favor fusion from a kinetic point of view), because the latter are already soft at 20 °C ($T_g \approx$ -50 °C)[33]. Importantly, as the monomer is quite soluble in water, MEA partitions between water and the particles. Therefore, the absolute concentration of MEA in the particles does not only depend on the wt%$_{MEA}$ (wt%$_{MEA}$ = $m_{free\ MEA}/(m_{free\ MEA} + m_{PMEA})$ = $m_{free\ MEA}/m_{total\ MEA}$), but also on the polymer concentration in the dispersion (*i.e.* the solids content). For highly diluted dispersions, it could thus be necessary to add much more MEA than to concentrated polymer dispersions in order to reach similar concentration of MEA in the micellar cores. Consistently, no noticeable change in particle size or turbidity were observed upon addition of 95 wt%$_{MEA}$ (corresponding to 2 vol%$_{MEA}$ in solvent) to highly diluted polymer dispersions (0.1 wt%), suggesting that no evolution happened. We believe that this phenomenon, along with the less likely collisions at low solids contents, might explain why only spheres are formed at low polymer content in many examples in the PISA literature[8,51,52]. While these preliminary experiments suggest that the total solids content also plays a role in the occurrence of morphological transitions, more work is required to fully elucidate the importance of this parameter.

In summary, in order to better understand what triggers morphological transitions during PISA, we have studied the formation of PDMAc-*b*-PMEA amphiphilic block copolymer nano-assemblies in a typical RAFT-PISA process. As expected, the final morphologies, *i.e.* the nano-objects formed at quasi-full monomer conversion, depend on the length of the PMEA core block. However, different morphologies were observed for the same PMEA block length depending on the conversion at which this length was reached, because the presence of MEA favors morphological transitions.

Through rheological analyses, we quantitatively assessed that the presence of free monomer, swelling the hydrophobic cores during the course of PISA, does not enhance, but, to our surprise, diminishes the rate of unimer exchange. Considering the time-scale of the polymerization, the intermediate self-assemblies must therefore be considered unable to reorganize by unimer exchange. We stress that although these results were obtained on one particular PISA system, this is sufficient to prove definitely that unimer exchange is not a prerequisite for morphological transitions in PISA. Considering that unimer exchange is too slow compared to the polymerization kinetics, the observed transitions to higher order morphologies (worms, vesicles) must be formed through fusion of primary spherical nano-objects. We however insist that this result does not imply that unimer exchange never occurs during PISA, nor that morphological transitions will not be observed in case unimer exchange is fast. Actually, fast unimer exchange should favor morphological transitions in PISA provided that the B block is long enough. Indeed, fast unimer exchange implies the formation of self-assembled structures at thermodynamic equilibrium, the morphology of which is dictated by the packing parameter, and therefore by the length of the B block.

Acknowledgements

This work has been funded by the Agence Nationale de la Recherche in the framework of the DYNAMIC-PISA ANR project (ANR-19-CE06-0002-01). The authors thank Gaëlle Pembouong and Claire Troufflard (IPCM) for their technical support, and Lazhar Benyahia and Cyrille Dechance (IMMM) for their help and support for the rheological measurements.

Keywords: block copolymer • micelles • vesicles • PISA • rheology

References

[1] F. D'Agosto, J. Rieger, M. Lansalot, *Angew. Chem. Int. Ed.* **2020**, *59*, 8368–8392.
[2] S. L. Canning, G. N. Smith, S. P. Armes, *Macromolecules* **2016**, *49*, 1985–2001.
[3] A. H. Milani, L. A. Fielding, P. Greensmith, B. R. Saunders, D. J. Adlam, A. J. Freemont, J. A. Hoyland, N. W. Hodson, M. A. Elsawy, A. F. Miller, L. P. D. Ratcliffe, O. O. Mykhaylyk, S. P. Armes, *Chem. Mater.* **2017**, *29*, 3100–3110.
[4] L. D. Blackman, S. Varlas, M. C. Arno, A. Fayter, M. I. Gibson, R. K. O'Reilly, *ACS Macro Lett.* **2017**, *6*, 1263–1267.
[5] T. Thambi, D. S. Lee, in *Stimuli Responsive Polym. Nanocarriers Drug Deliv. Appl.* (Eds.: A.S.H. Makhlouf, N.Y. Abu-Thabit), Woodhead Publishing, **2019**, pp. 413–438.
[6] F. Coumes, F. Stoffelbach, J. Rieger, in *Macromol. Eng.*, John Wiley & Sons, Ltd, **2022**, pp. 1–84.
[7] J. N. Israelachvili, *Intermolecular and Surface Forces - 3rd Edition*, Acad. Press: Amsterdam, **2011**.
[8] S. Sugihara, A. H. Ma'Radzi, S. Ida, S. Irie, T. Kikukawa, Y. Maeda, *Polymer* **2015**, *76*, 17–24.
[9] C. A. Figg, A. Simula, K. A. Gebre, B. S. Tucker, D. M. Haddleton, B. S. Sumerlin, *Chem. Sci.* **2015**, *6*, 1230–1236.
[10] F. Coumes, M. Balarezo, J. Rieger, F. Stoffelbach, *Macromol. Rapid Commun.* **2020**, *41*, 2000002.
[11] M. Chenal, L. Bouteiller, J. Rieger, *Polym. Chem.* **2013**, *4*, 752–762.
[12] J. Rieger, *Macromol. Rapid Commun.* **2015**, *36*, 1458–1471.
[13] V. J. Cunningham, A. M. Alswieleh, K. L. Thompson, M. Williams, G. J. Leggett, S. P. Armes, O. M. Musa, *Macromolecules* **2014**, *47*, 5613–5623.
[14] N. P. Truong, M. V. Dussert, M. R. Whittaker, J. F. Quinn, T. P. Davis, *Polym. Chem.* **2015**, *6*, 3865–3874.

[15] D. Ikkene, A. A. Arteni, M. Ouldali, J.-L. Six, K. Ferji, *Polym. Chem.* **2020**, *11*, 4729–4740.
[16] L. D. Blackman, K. E. B. Doncom, M. I. Gibson, R. K. O'Reilly, *Polym. Chem.* **2017**, *8*, 2860–2871.
[17] S. Y. Khor, N. P. Truong, J. F. Quinn, M. R. Whittaker, T. P. Davis, *ACS Macro Lett.* **2017**, *6*, 1013–1019.
[18] A. Czajka, S. P. Armes, *Chem. Sci.* **2020**, *11*, 11443–11454.
[19] J. Y. Rho, G. M. Scheutz, S. Häkkinen, J. B. Garrison, Q. Song, J. Yang, R. Richardson, S. Perrier, B. S. Sumerlin, *Polym. Chem.* **2021**, *12*, 3947–3952.
[20] T. Nicolai, O. Colombani, C. Chassenieux, *Soft Matter* **2010**, *6*, 3111.
[21] A. Halperin, S. Alexander, *Macromolecules* **1989**, *22*, 2403–2412.
[22] G. Landazuri, V. V. A. Fernandez, J. F. A. Soltero, Y. Rharbi, *Macromolecules* **2021**, *54*, 2494–2505.
[23] E. J. Cornel, G. N. Smith, S. E. Rogers, J. E. Hallett, D. J. Growney, T. Smith, P. S. O'Hora, S. van Meurs, O. O. Mykhaylyk, S. P. Armes, *Soft Matter* **2020**, *16*, 3657–3668.
[24] R. Lund, L. Willner, J. Stellbrink, D. Richter, *Phys. B Condens. Matter* **2006**, *385–386*, 735–737.
[25] D. Bendejacq, M. Joanicot, V. Ponsinet, *Eur. Phys. J. E* **2005**, *17*, 83–92.
[26] M. Jacquin, P. Muller, R. Talingting-Pabalan, H. Cottet, J. F. Berret, T. Futterer, O. Théodoly, *J. Colloid Interface Sci.* **2007**, *316*, 897–911.
[27] E. J. Cornel, P. S. O'Hora, T. Smith, D. J. Growney, O. O. Mykhaylyk, S. P. Armes, *Chem. Sci.* **2020**, *11*, 4312–4321.
[28] Y. Rharbi, M. A. Winnik, K. G. Hahn, *Langmuir* **1999**, *15*, 4697–4700.
[29] E. Villar-Alvarez, S. Barbosa, J. F. A. Soltero, V. Mosquera, P. Taboada, Y. Rharbi, *J. Phys. Chem. C* **2018**, *122*, 8553–8563.
[30] G. Liu, Q. Qiu, W. Shen, Z. An, *Macromolecules* **2011**, *44*, 5237–5245.
[31] G. Mellot, J.-M. Guigner, L. Bouteiller, F. Stoffelbach, J. Rieger, *Angew. Chem.* **2019**, *131*, 3205–3209.
[32] W. Steinhauer, R. Hoogenboom, H. Keul, M. Moeller, *Macromolecules* **2013**, *46*, 1447–1460.
[33] M. Tanaka, T. Motomura, N. Ishii, K. Shimura, M. Onishi, A. Mochizuki, T. Hatakeyama, *Polym. Int.* **2000**, *49*, 1709–1713.
[34] N. Coudert, C. Debrie, J. Rieger, T. Nicolai, O. Colombani, *Macromolecules* **2022**, *55*, 10502–10512.
[35] "Specialty Chemicals home pages | FUJIFILM Wako Pure Chemical Corporation," can be found under https://specchem-wako.fujifilm.com/asia/, **2022**.
[36] L. A. Fielding, M. J. Derry, V. Ladmiral, J. Rosselgong, A. M. Rodrigues, L. P. D. Ratcliffe, S. Sugihara, S. P. Armes, *Chem. Sci.* **2013**, *4*, 2081–2087.
[37] S. J. Byard, M. Williams, B. E. McKenzie, A. Blanazs, S. P. Armes, *Macromolecules* **2017**, *50*, 1482–1493.
[38] In *Intermolecular Surf. Forces - 3rd Ed.*, Acad. Press: Amsterdam, **2011**, pp. 535–576.
[39] T. Annable, R. Buscall, R. Ettelaie, D. Whittlestone, *J. Rheol.* **1993**, *37*, 695–726.
[40] C. Chassenieux, T. Nicolai, L. Benyahia, *Curr. Opin. Colloid Interface Sci.* **2011**, *16*, 18–26.
[41] T. Zinn, L. Willner, R. Lund, *ACS Macro Lett.* **2016**, *5*, 1353–1356.
[42] K. Halperin, J. B. Ketterson, P. Dutta, *Langmuir* **1989**, *5*, 161–164.
[43] D. Danino, D. Weihs, R. Zana, G. Orädd, G. Lindblom, M. Abe, Y. Talmon, *J. Colloid Interface Sci.* **2003**, *259*, 382–390.
[44] N. P. Truong, J. F. Quinn, A. Anastasaki, D. M. Haddleton, M. R. Whittaker, T. P. Davis, *Chem. Commun.* **2016**, *52*, 4497–4500.
[45] K. Parkatzidis, N. P. Truong, M. Rolland, V. Lutz-Bueno, E. H. Pilkington, R. Mezzenga, A. Anastasaki, *Angew. Chem.* **2022**, *134*, e202113424.
[46] G. Bovone, L. Cousin, F. Steiner, M. W. Tibbitt, *Macromolecules* **2022**, 9.
[47] V. Lohmann, M. Rolland, N. P. Truong, A. Anastasaki, *Eur. Polym. J.* **2022**, *176*, 111417.
[48] M. Rolland, N. P. Truong, K. Parkatzidis, E. H. Pilkington, A. L. Torzynski, R. W. Style, E. R. Dufresne, A. Anastasaki, *JACS Au* **2021**, *1*, 1975–1986.
[49] M. Rolland, E. R. Dufresne, N. P. Truong, A. Anastasaki, *Polym. Chem.* **2022**, *13*, 5135–5144.
[50] S. Boissé, PhD thesis, Université Paris 6, **2010**.
[51] A. Blanazs, A. J. Ryan, S. P. Armes, *Macromolecules* **2012**, *45*, 5099–5107.
[52] N. J. Warren, S. P. Armes, *J. Am. Chem. Soc.* **2014**, *136*, 10174–10185.

† The results displayed in ***Figure 3a*** have also been reported in our related paper[34], highlighting the influence of temperature and the B block length x on the relaxation time. In the same paper, we additionally demonstrated that above a critical temperature T_c (which decreases with x) the physical networks reorganize, preventing any quantitative measurement in these conditions because the rheological properties slowly evolve with time. Still, the reorganization above T_c tends to increase the rheological relaxation time, implying that the values determined below T_c represent minimum values of the exchange time.

‡ The very first morphological transition, from spheres to short worms, actually occurred somewhere between $DP_{n,B}$ = 70 and 107. In these conditions, the role of unimer exchange cannot be fully excluded although it is unlikely (τ_r is already between 10^1 s and more than 10^3 s for this DP_n-range even in the absence of monomer). For the subsequent transitions, unimer exchange is definitely excluded. Indeed, these transitions occur between 25% and 50% conversion, that is within less than 1h, which corresponds on average to the time needed for one unimer-exchange event.

Entry for the Table of Contents

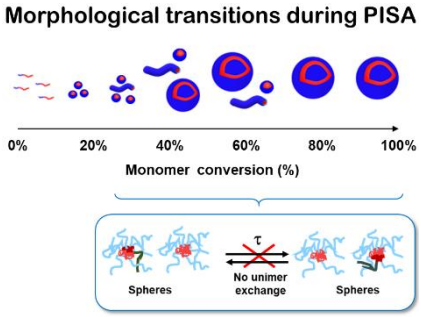

We demonstrate that morphological transitions during radical RAFT-mediated PISA in water do not require unimer exchanges and that the monomer present in the polymerization medium enables morphological transitions although it unexpectedly slows down unimer exchange.

Institute Twitter usernames: @IPCM_Sorbonne; @Sorbonne_Univ_; @CNRS; @LeMansUniv; @IMMM_UMR_6283